Proceedings of the American Control Conference
San Diego, California • June 1999

Dynamics and Control of Micromachined Gyroscopes

Andrei M. Shkel[♮], Roberto Horowitz[♯], Ashwin A. Seshia[♮], Sungsu Park[♯], and Roger T. Howe[♮♯]

Berkeley Sensor & Actuator Center
[♮]Department of Electrical Engineering and Computer Sciences
[♯] Department of Mechanical Engineering
University of California at Berkeley
Berkeley, California 94720

Abstract

In this paper we summarize principles of operation of micromachined gyroscopes, analyze dynamics of ideal and non-ideal systems, and propose an approach for formulation and solving problems of control. The suggested approach uses active non-linear feedback control for drive and compensation of errors. Both non-adaptive and adaptive strategies are presented. These strategies can be used for a broad class of micromachined vibratory gyroscopes including those for angle and angular rate measurement. Control approaches described in this paper are in the implementation stage and will soon be tested on gyroscope prototypes.

1 Introduction

Gyroscopes are the most commonly used devices for measuring angular velocity and angular rotation in many navigation, homing, and stabilization applications. Over the past several decades many different gyroscope concepts have been developed. Recent advances in silicon micromachining technology have raised the possibility of revolutionizing the field of inertial instruments by providing inexpensive, miniature gyroscopes, to address market needs for low-cost medium performance inertial instruments. Micromachined accelerometers have been extremely successful in high volume and low-cost automotive applications such as air bags, vehicle stabilization systems and active suspensions. Micro-gyroscopes are projected to exhibit similar success. However, the dynamics of micromachined gyroscopes is much more complicated than that of most micromachined accelerometers. The later are generally one degree of freedom systems while the former have to be modeled by a multi-degree of freedom coupled differential equations.

Micromachined gyroscopes are probably the most challenging type of transducers ever attempted to be designed in micro-world. A nail size dynamic system integrated with control electronics on the same silicon chip (Fig.1) is designed to be a very sensitive sensor which is able to detect maneuvers and motions which are even beyond human perception abilities. Along with exciting opportunities which MEMS gyroscopes could bring to our everyday life, the miniaturization introduces many technical challenges. Multi-degree of freedom dynamics, sensitivity to fabrication imperfections, dynamic instability, limited control resources - all these raise a number of fundamentally complicated issues in the design, analysis, and control of micromachined gyroscopes. In this paper we discuss some of these issues and propose an approach for formulation and solving problems of control.

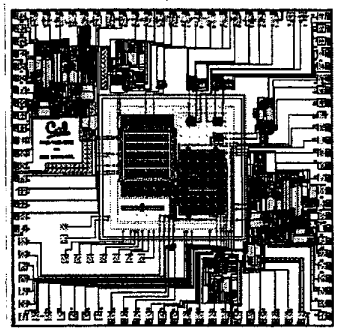

Figure 1: Layout of integrated gyro module (5mm × 5mm). Includes two gyroscopes (center) and on-chip control electronics. The chip is being fabricated in Sandia's iMEMS technology.

2 Basics of Micromachined Gyroscopes

In most micromachined gyroscope designs the vibrating angular rate sensor consists of a mass suspended on elastic flexures anchored to the substrate. This mass is constrained to vibrate on one of the planes: x-y plane in case of the z-axis gyroscope[1] or y-z plane in case of the x-axis gyroscope (e.g., [2]). The x-axis and y-axis form a plane parallel to the substrate and the z-axis is perpendicular to the substrate, Fig.2. In this

paper, without lost of generality, we refer to the z-axis gyroscope, however, all results are directly applicable to gyroscopes with x- and y-axis of sensitivity.

2.1 Dynamics

To describe dynamics of the gyroscope, it is convenient to intoduce two coordinate systems: $\{\xi, \eta, \zeta\}$ - inertial, fixed in an absolute space, and $\{x, y, z\}$ - non-inertial, rigidly attached to the platform. Angular velocity $\vec{\Omega} = (\Omega_x, \Omega_y, \Omega_z)$ of the platform is associated with angular velocity of the object to which the gyroscope is attached.

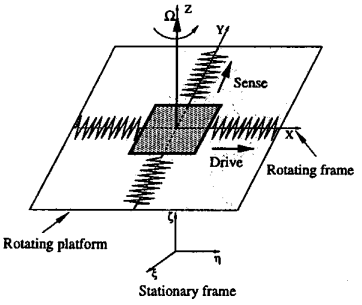

Figure 2: Mass-spring model of the vibratory micromachined gyroscope.

The behavior of the gyroscope is naturally described with respect to the non-inertial coordinate frame $\{x, y, z\}$. When equations of motion are written with respect to this frame, the "fictitious" or "inertial forces" has to be treated as actual physical forces. The second Newton Law then has the form $m\vec{a}_{xyz} = \vec{F}_{ext} - m\vec{a}_e - m\vec{a}_c$. Here, $\vec{a}_{xyz}$ is a linear acceleration of the gyroscope with respect to the coordinate frame $\{x, y, z\}$, $\vec{F}_{ext}$ is a sum of all external forces acting on the proof mass (including elastic restoring forces, damping, etc.), $\vec{a}_e$ is centrifugal acceleration which is a function of Ω^2 and $\dot{\vec{\Omega}}$, and $\vec{a}_c$ is the Coriolis acceleration.

For traditional inertial navigation applications the rotation rate is small relative to the natural frequency of the system and is also constant over a relatively long time interval. Also, linear acceleration terms can be typically cancelled out as an offset from the output response. In addition, if we are interested in measuring the rotation rate about only the z-axis (Fig. 2), then it is possible to make the stiffness in the z-direction much larger than the stiffness in the other two orthogonal directions through special fabrication techniques and careful design. If all these requirements are satisfied, all inertial forces, except the Coriolis force, can be ignored and the governing equations in Cartesian coordinates $\{x, y, z\}$ are given by

$$\ddot{x} + \omega_n^2 x - 2\Omega\dot{y} = 0$$

$$\ddot{y} + \omega_n^2 y + 2\Omega\dot{x} = 0 \qquad (1)$$

The essential feature of these equations is the presence of the Coriolis acceleration terms $-2\Omega\dot{y}$ and $2\Omega\dot{x}$. These two terms will appear only if the equations of motion are written in a non-inertial coordinate frame. It is the Coriolis acceleration that causes a transfer of energy between two of the gyroscope modes of operation (Fig. 3).

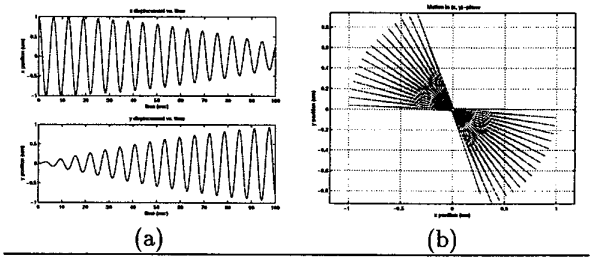

Figure 3: The Coriolis acceleration causes the precession of the line of oscillation. The oscillating proof mass is intending to keep the line of oscillation constant in the absolute space; this effect is equivalent to the transfer of energy between two of the gyroscope modes of operation in a non-inertial coordinate frame.

If the "input" angular velocity Ω is zero, and under appropriate initial conditions, the ideal gyroscope will oscillate along a straight line. The orientation of the straight line is defined by initial conditions. In a more general case, when the initial conditions are such that the vector of displacement is not parallel to the vector of velocity, the "orbit" of the gyroscope motion is an ellipse. The general solution of (1) then, for the case when $\Omega = 0$, is

$$x = A\cos(\omega_n t + \theta_0)\cos\phi - B\sin(\omega_n t + \theta_0)\sin\phi$$
$$y = A\cos(\omega_n t + \theta_0)\sin\phi + B\sin(\omega_n t + \theta_0)\cos\phi$$

The parameters A, B, ϕ, and θ_0 are constants defined by the initial conditions: a and b define the shape of the ellipse, ϕ - orientation of the ellipse, and θ_0 defines location of the gyroscope reference point on the ellipse at the initial instant.

2.2 Principle of Operation

The vibratory gyroscopes can operate in two different modes: the angle and the angular rate modes. Regardless of the mode of gyroscope operation, the best performance is achieved when the stiffness is same in all direction, or the system is isotropic. When the isotropic oscillator is allowed to freely oscillate, the precession of the straight line of oscillation provides a measure of the angle of rotation (Fig. 3). The angle of the precessing pattern can be instantly defined from the

measurements of the vector of displacement and velocity [3]:

$$\tan\phi = \frac{2(\omega_n^2 xy + \dot{x}\dot{y})}{\omega_n^2(x^2 - y^2) + (\dot{x}^2 - \dot{y}^2)} \quad (2)$$

To measure rotation rate, the proof-mass would be driven to a fixed amplitude along the x-axis by applying an electrostatic drive force to the proof-mass along the x-axis. In the absence of rotation there would be no motion of the proof-mass along the y-axis. Under rotation, however, the Coriolis acceleration will cause energy to be transferred from the x-axis (primary mode) to the y-axis (secondary mode) building up vibration amplitude along the y-axis. The ratio of the amplitude in the secondary mode vibration to the amplitude of the primary mode vibration can be shown to be proportional to the rotation rate and is given by (e.g., [4])

$$\frac{y}{x} = 2Q\frac{\Omega}{\omega_n} \quad (3)$$

Notice, that the gyroscope response is proportional to quality factor Q of the gyroscope. If the quality factor is not changing, the rotation rate can be determined by simply measuring the amplitude of the secondary mode. Rotation rate can be measured in by operating the gyroscope in either the open-loop or the closed-loop (force-to-rebalance) modes. The force-to-rebalance control loop operates exactly like the amplitude control in the drive direction. Only in this case, the secondary mode amplitude is continuously driven to zero rather than a fixed value.

2.3 Non-ideal Gyroscope

Fabrication of micromachined gyroscopes involves multiple processing steps including the deposition, etching, and patterning of materials. Depending on the technology, different number of steps is involved and different fabrication tolerances can be achieved at each step. As a rule, every fabrication step contribute to imperfections in the gyroscope. In practice, imperfections are reflected in asymmetry and anisoelasticity of the structure. Consequently, asymmetries result in undesirable constantly acting perturbations in the form of mechanical and electrostatic forces.

The governing equations of a non-ideal gyroscope in Cartesian coordinates $\{x, y, z\}$ are given by

$$M\ddot{q} + D\dot{q} + Kq + 2\Gamma\dot{q} = F \quad (4)$$

where M is a matrix of mass distribution, $q = (x, y)^T$ is the displacement of the gyroscope's reference point, and $F = (F_x, F_y)^T$ is the control input. In presence of imperfections stiffness and damping have the form

$$D = \begin{bmatrix} d_{xx} & d_{xy} \\ d_{yx} & d_{yy} \end{bmatrix}, \quad K = \begin{bmatrix} \omega_n^2 & c_{xy} \\ c_{yx} & \omega_n^2 \end{bmatrix}$$

The essential part of the equation is the Coriolis force which is defined by the skew-symmetric matrix

$$\Gamma = \begin{bmatrix} 0 & -\Omega \\ \Omega & 0 \end{bmatrix}$$

For any two dimensional system of springs, no matter how complex, we can uniquely define two principal spring axes (or main axes of elasticity) and corresponding equivalent spring constants. The off-diagonal elements in the stiffness matrix appear when the main axes of elasticity do not coincide with the coordinate system {x y}. By analogy with stiffness, damping can also be described in terms of two main axes of damping. In general, the principal axes of elasticity and damping are not necessarily aligned because asymmetry in stiffness and damping are caused by different physical phenomena. Thus, off-diagonal elements in the damping matrix are also appear due to misalignment of the main axes of damping with the coordinate axes x and y [5].

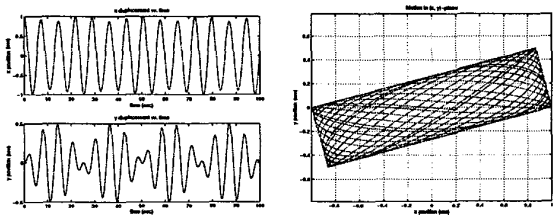

Figure 4: Off-diagonal elements in the stiffness matrix result in frequency change and disruption of the straight line oscillation. (Left) time response along x−axis and y−axis; (Right) (x,y) plane response

Off-diagonal elements in the stiffness matrix result in frequency change and disruption of the straight line oscillation, Fig.4. (The ideal system is supposed to oscillate along a horizontal straight line with constant amplitude and frequency). The off-diagonal symmetric elements in the damping matrix result in precession of the straight line oscillation and amplitude change. On the other hand, skew-symmetric terms in the damping matrix cause only precession of the gyroscope line of oscillation. The effect of off-diagonal damping elements is not distinguishable from the effect of the Coriolis force, and thus present significant difficulties for their compensation. Perturbations proportional to the velocity can appear as a result of losses due to structural damping, transmission of energy to suspension, aerodynamic drag, etc. Gyroscopic forces (skew-symmetric terms in damping matrix) can appear only as inertial forces or as a side effect of an active control. The general classification scheme on influence of defects on gyroscope behavior is presented in [5].

3 Gyroscope Control

The gyroscope control system performs four basic tasks: (1) initiates oscillations until the appropriate energy level is reached; (2) maintains the reached energy level; (3) compensates for quadrature deviation from the reference straight line of oscillations; (4) senses displacements and velocities in a pair of orthogonal directions.

Traditionally, tasks (1) and (2) are solved by driving a micro-machined structure at resonance. This is typically done by employing a transresistance amplifier configured in positive feedback [6]. The oscillation amplitude can be kept constant using an automatic gain control loop. The task (4) can be solved using lateral and diffrenetial comb fingers. The lateral interdigitated comb fingers [7] can be used to measure linear velocity of the proof-mass and parallel plate capacitive arrangements can be used to measure deflection of the structure (practical examples of arrangements are reviewed in [8]). Traditional quadrature error cancellation, task (3), cannot be easily extrapolated to mode matched gyroscopes and is dependent on exact phase relations between signals corresponding to displacement and velocity in the two orthogonal directions [1]. In this paper we propose a more general approach which treats the gyroscope as a multi-degree of freedom device and compensates for a general class of quadrature errors and energy losses. Among advantages of the proposed control strategies are their universal applicability to different gyroscope designs, robust quadrature cancellation scheme, feedback compensation of energy dissipation, and on-line parameter tuning.

3.1 Definition of Quadrature

Ideally, the gyroscope oscillates along a straight line and the Coriolis force causes the precession of this straight line, the precession is detected and information about the angle or angular rate is extracted. Nonidealities in the gyroscope, such as misalignment of the drive forces and anisoelasticity can cause ellipticity of the nominal straight line motion. Ellipticity of the gyroscope trajectory is undesirable because it directly enters into the measurements. Thus, as a general rule, zero ellipticity is desirable. Angular momentum $[(\dot{x},\dot{y})^T \times (x,y)^T]$ or ellipticity (quadrature) are good measures of deviation from a straight line oscillations:

$$\begin{aligned} P &= \frac{1}{2}\oint(xdy - ydx) = \frac{1}{2}\int_0^{2\pi}(x\dot{y} - y\dot{x})dt \\ &= \pi(x\dot{y} - y\dot{x}) \end{aligned} \tag{5}$$

This measure of quadrature P will be used for defining a quadrature compensating controller. With some precautions discussed in the next section, the general goal of the quadrature control is to drive the area of the quadrature ellipsoid (5) to zero.

3.2 General Control Strategy

The gyroscope is sensitive to uncompensated defects which can arise due to the nature of the fabrication process, parasitic electrostatic forces and unwanted electrostatic cross coupling. These defects manifest themselves as unwanted terms in the spring and damping matrix. For example, symmetric off-diagonal terms in the stiffness matrix can cause the evolution of motion to be a precessing ellipsoid instead of a straight line, Figure 5(a). Therefore, the Coriolis force induced amplitudes along the x- and y-axis no longer give us the correct information about the rotation rate.

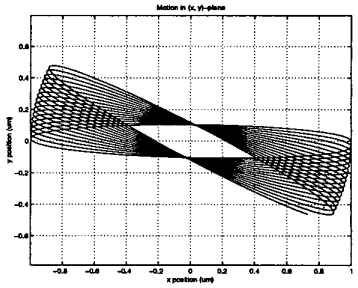

(a)

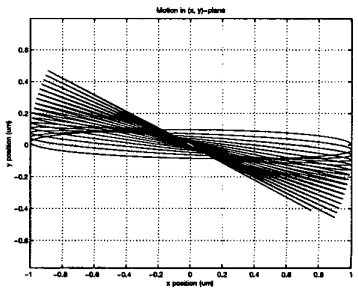

(b)

Figure 5: Performance of control minimizing quadrature. (a) The ellipsoid defining the quadrature precesses due to the Coriolis force; no control applied; (b) The area of quadrature ellipsoid converges to zero while the line of oscillation continue to precess; active feed-back control (6) is applied

At the same time this control should not interfere with the Coriolis force. Based on the result of classification of errors [5], the topology of the controller which will not interfere with the Coriolis force, while compensating for the quadrature, should have the form

$$F_{quadr} = -\gamma_1 \cdot P \cdot S^T \cdot q \tag{6}$$

Here, γ_1 is a constant gain, P is quadrature defined by (5), S is a skew-symmetric matrix, and q is a displacement vector. This non-linear feedback control stabilizes the system to a manifold in the gyroscope phase space; the manifold corresponds to the straight line seg-

ment in (x,y)-plane. The performance of the quadrature compensation controller is illustrated in Fig. 5. In result of the quadrature control action, the area of the quadrature ellipsoid converges to zero, i.e. the ellipsoid approaches a straight line. Notice also that the quadrature control does not effect the rate of the precession.

In addition to such a control, one often uses an additional control to maintain constant overall energy of the system so that damping and other dissipative effects can be compensated. The deviation of the actual energy level of the system from the nominal can be defined by

$$\Delta E = E_o - \frac{\omega_n^2(x^2+y^2)+(\dot{x}^2+\dot{y}^2)}{2} \tag{7}$$

where E_o denotes the nominal energy of the system normalized with respect to the effective mass. A control which will not interfere with the Coriolis force and will force the system to maintain the nominal energy level has the form:

$$F_{energy} = -\gamma_2 \cdot \Delta E \cdot \dot{q} \tag{8}$$

This control force is proportional to the velocity and acts to cancel out the damping effects. Even though it is designed for angle masuring gyroscope, it can be easily adapted for use in rate gyroscopes.

In most gyroscope designs, it is also important to match fundamental frequencies of the system. This can be done, for example, by driving the average frequency to the nominal one

$$\Delta\omega = \omega_n - \frac{\omega_x+\omega_y}{2} \tag{9}$$

The goal can be accomplished with the control

$$F_{tuning} = -\gamma_3 \cdot \Delta\omega \cdot q \tag{10}$$

Spherical potential forces (10) can only cause frequency change in the system and do not contribute to any other changes in the system. This insures that the control (10) will not interfere with the Coriolis signal and will drive the frequency mismatch (9) to zero. The tuning control is a very important element in design of angular rate transducers because frequency mismatch directly defines the sensitivity of the device.

When a gyroscope operates as an angle measuring transducer, it should be allowed freely precess in response to the Coriolis force - no feedback strategies for compensation of precession can be effectively employed. However, the rate measuring gyroscope can operate in two different modes: the open-loop mode and the force-to-rebalance mode. In the closed-loop mode, the secondary mode amplitude is continuously monitored and driven to zero by applying the appropriate drive force to the proof-mass along the y-axis (e.g., see [4]). In this case, the force-to-rebalance control should be integrated with all three control loops described above: quadrature, energy, and frequency tuning.

In summary, it can be concluded that one of the necessary conditions for gyroscope operation is the stability of the nominal harmonic motion of the device and its insensitivity to the external perturbations. Three coordinated feedback control actions are designed: the first is the control that minimizes quadrature errors, equation (6); the second compensates for the energy variations, equation (8); and the third tunes the frequencies of the system to a desirable value, equation (10). All three controls are designed to compensate for manufacturing defects and electrostatic interferences. The distinguishing feature of these controls is that they do not interfere with the measured Coriolis signal while performing assigned tasks.

3.3 Adaptive Control

The stiffness tuning described by (10) can be alternatively accomplished using an adaptive control scheme. The adaptive control scheme can also provide a good estimation of the angular velocity.

We post the following problem: find a control strategy which will drive the non-ideal system (4) to an ideal:

$$\ddot{q} + \omega_n^2 q = 0 \tag{11}$$

while provides stiffness tuning, compensation for damping, and estimation of the angular velocity.

To solve this problem, we build the adaptive controller which is based on quadrature and energy compensation, F_{quadr} and control compensating for energy losses F_{energy} defined by (6) and (8), respectively. Denote the sum of these two controllers by $F_1 = F_{quadr} + F_{energy}$, then the parameter estimation algorithm has the form

$$\begin{aligned} \dot{\hat{\Gamma}} &= \gamma_\Omega\{F_1\dot{q}^T - \dot{q}F_1^T\} \\ \dot{\hat{K}} &= \frac{1}{2}\gamma_K\{F_1 q^T + qF_1^T\} \end{aligned} \tag{12}$$

and the corresponding adaptive controller is given by

$$F_2 = \hat{K}q + 2\hat{\Gamma}\dot{q} \tag{13}$$

In (12) and (13), $\hat{K}$ and $\hat{\Gamma}$ are estimated values of damping, stiffness, and angular velocity, respectively.

If damping D is known and can be compensated, than it can be shown that the controller $F = F_1 + F_2$ guarantees that the stiffness converges to the desirable value (i.e., frequency tuning is accomplished) and the estimation of the angular velocity $\hat{\Omega}$ converges to the actual value of the angular velocity Ω, Fig. 6.

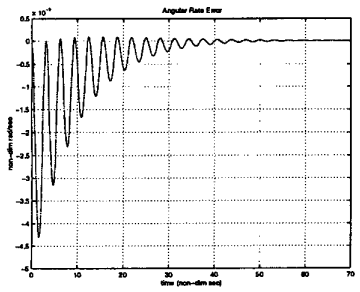

Figure 6: Convergence of the angular rate estimation to the actual value. After 70 non-dimensional seconds (in time scale of the natural frequency) the ratio between estimated and the actual values is less than 3 %.

It should be noted, however, that if off-diagonal elements in the damping matrix D are unknown, the effect caused by these elements to the change in dynamics of the system is not distinguishable from the Coriolis force and will enter into the estimation of angular velocity as an additional bias. Due to space limitations, the proof of convergence and strategy for estimation of unbiased angular velocity are omitted and will appear elsewhere.

4 Conclusions

In this paper we studied issues of dynamics and control of micromachined vibratory gyroscopes and found that vibratory gyroscopes are inherently unstable systems which are extremely sensitive to defects, imperfections, and undesirable perturbations. Vibratory micromachined gyroscopes should no doubt include a feedback control system to maintain the amplitude of oscillation constant and keep the ellipticity of the gyroscope trajectory small (i.e., drive the area of quadrature to zero). The essential requirement is that these tasks have to be accomplished while avoiding interference with the measured Coriolis acceleration. This is the necessary condition for gyroscope control.

The analysis presented in the paper shows that, under certain conditions, the nonlinear feedback controller which includes quadrature control Eq.(6), energy control Eq.(8), and frequency tuning Eq.(10) can be utilized to stabilize the behavior of the gyroscope while providing no interference with the coriolis signal. Also, if the adaptive extension (13) is used, additional frequency tuning and closed-loop angular velocity estimation options are available. It is also concluded, that the limitation of any feedback control system is its lack of ability to compensate for the Coriolis-like defects and perturbations. Thus, each gyroscope should include a calibration unit for identification and compensation of defects which cannot be compensated with the active control.

In summary, the proposed nonlinear feedback control stabilizes the system, allows multi-directional vibrations of the gyroscope, and does not interfere with the Coriolis acceleration. This control architecture with slight modifications can be universally applied to angular rate and angle measuring gyroscopes. The control will be implemented on a chip integrated with other conditioning loops. The implementation will be carried out in both polysilicon surface micromachining and silicon-on-insulator (SOI) technologies.

5 Acknowledgments

The first author is grateful to faculty of the department of Applied Mechanics and Control of Moscow State University for useful discussions on earlier stages of this work.

References

[1] William A. Clark, Roger T. Howe and Roberto Horowitz. Surface micromachined z-axis vibratory rate gyroscope. *IEEE Solid State Sensors and Actuators Workshop*, pages 283–287, June 1996. Hilton Head Island, SC.

[2] Jon Bernstein et al. A micromachined comb-drive tuning fork rate gyroscope. *Micro Electro Mechanical Systems*, pages 143–148, February 1993. Fort Lauderdale, Florida.

[3] Victor F. Juravlev and Dmitrii M. Klimov. *"Solid-State Wave Gyroscope"*. Nauka, Moscow, 1985. (in Russian).

[4] Michael W. Putty and Khalil Najafi. A micromachined vibrating ring gyroscope. *IEEE Solid State Sensors and Actuators Workshop*, pages 213–220, June 1994. Hilton Head Island, SC.

[5] Andrei M. Shkel, Roger T. Howe, and Roberto Horowitz. Modeling and simulation of micromachined gyroscopes in the presence of imperfections. *Intern. Conf. On Modeling and Simulation of Microsystems (MSM'99)*, April 1999. Puerto Rico, U.S.A. (To appear).

[6] Clark T. Nguyen and Roger T. Howe. CMOS micromechanical resonator oscillator. *Technical Digest, IEEE International Electron Devices Meeting*, pages 199–202, 1993. Washington, DC.

[7] William C. Tang, Clark T. Nguyen, and Roger T. Howe. Laterally driven polysilicon resonant microstructures. *Sensor and Actuator*, 20:25–32, 1989.

[8] Larry K. Baxter. *"Capacitive Sensors"*. IEEE Press, 1997.